2024 IEEE International Conference on Robotics and Automation (ICRA 2024)
May 13-17, 2024. Yokohama, Japan

LeagTag: An Elongated High-Accuracy Fiducial Marker for Tight Spaces*

Hideyuki Tanaka[1] and Kunihiro Ogata[2]

Abstract— **Fiducial markers enable reliable service robot control. In human-robot coexistence environments, efficient placement of square or circular markers can be challenging due to limited space. In this study, we developed a world-first, elongated fiducial marker, capable of high-accuracy 6-DoF measurements, designed to be installable in tight spaces. We introduced two types of lenticular angle gauges to enhance pose estimation and developed new marker patterns and measurement algorithms to maintain recognition distance and accuracy. The proposed marker achieved a measurement accuracy of 0.1% position error and 0.5° orientation error. This technology will enhance the practicality and applicability of fiducial markers, contributing to the creation of robot-friendly space for future service robots.**

I. INTRODUCTION

A fiducial marker is a planar pattern that can estimate its pose (position and orientation) in the camera coordinate system by capturing it with a monocular camera. Various types of fiducial markers, such as ARToolKit [1], RUNE-Tag [2], AprilTag [3], ChromaTag [4], and ArUco [5], have been developed, providing a simple and reliable method for 6-DoF measurements. They are still widely used in various fields of robotics, including calibration [6][7], manipulation [8][9], localization [10][11], and navigation [12][13], despite the recent development of object recognition and 3-D measurement technologies based on deep learning.

Specifically, service robots are expected to see increased use in human-robot coexistence environments [14]. Therefore, we must adapt fiducial markers to such environments. Two physical challenges arise here: (1) markers can be visually obtrusive, and (2) available space for markers is often limited. To address the first issue, there are some methods of making the markers less visible [15][16]. However, we are considering making them visible but compact, enabling human use similar to QR codes for potential future services.

The primary focus of this study is to tackle the second issue (2). In human-robot coexistence environments, there are not many flat surfaces that are moderately spacious and suitable for placing fiducial markers. For instance, in a future convenience store where a mobile manipulator handles products on shelves [17], where should the markers be placed to support accurate pose detection and alignment? In this case, the only option is to place the markers on the front surface of the shelves or the frame, both of which are narrow areas. Conventional fiducial markers are typically square or circular in shape. When placed in narrow areas, markers with a 1:1 aspect ratio become small in both dimensions, resulting in unnecessary reductions in marker recognition distance and measurement accuracy. The crucial point is that simply creating a long rectangular marker or arranging multiple square markers in a row does not address these issues due to the presence of short sides.

In this study, we have undertaken the development of elongated markers for efficient placement in tight spaces, avoiding unnecessary performance degradation. We designed a new marker, developed a prototype, and created recognition and measurement algorithms to maximize its performance.

Although markers for curved surfaces [18] and free-form shapes [19] have been developed, there are no existing examples of markers that can be installed in narrow spaces with both high accuracy and an elongated shape. Our developed marker represents the world's first of its kind. We believe our technology will contribute to enhancing the practicality and applicability of fiducial markers in robotic aplications.

The paper first describes the marker design, including the background technology. Next, it outlines the recognition and measurement algorithms of the marker, followed by the presentation of performance verification results.

II. MARKER DESIGN

In this section, we will explain the design process for the marker we developed. To facilitate the explanation, we will first introduce the developed prototype of the marker.

A. Appearance and Components of Developed Marker

We show the developed prototype of the marker in Fig. 1. The most notable feature of the marker is its elongated rectangular shape with an aspect ratio of 5.6:1. It consists of two 2-D codes, four feature dots, and two types of LEAGs. "LEAG" is an abbreviation for "lenticular angle gauge"

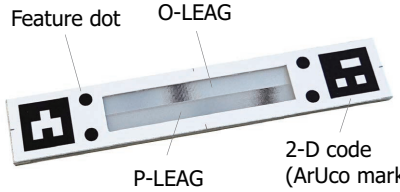

Fig. 1. Prototype of the developed fiducial marker, with dimensions of 75.5x13.6x1.5 mm, was created by attaching a LEAG sheet onto a cardboard sheet, and then overlaying it with a black-and-white patterned paper that had an opening designed for the LEAG.

*This work was supported by JSPS KAKENHI Grant No. JP21H03471, and is based on results obtained froma a project, JPNP14004, commissioned by NEDO.

[1]Hideyuki Tanaka and [2]Kunihiro Ogata are with Human Augmentation Research Center, National Institute of Advanced Industrial Science and Technology, Kashiwa, Chiba, Japan. hideyuki-tanaka@aist.go.jp, ogata.kunihiro@aist.go.jp

and is an important element that enables high orientation estimation accuracy. We named the elongated fiducial marker we developed "LeagTag." The description of each component will be provided in the following subsections.

B. LEAG

Conventional fiducial markers use the PnP (perspective-n-point) method [20][21] to determine camera-to-marker transformations by extracting known feature points. However, this approach can result in pose estimation inaccuracies, particularly when dealing with small markers or frontal views [22], a common limitation of conventional markers

In 2012, the author introduced LentiMark [23], a high-accuracy fiducial marker with a novel attitude measurement principle. LentiMark employed two LEAGs, special lens components with a moving black line that correlates with the viewing angle, to extract precise attitude information. This innovation enabled stable attitude estimation, even with small markers and frontal observations, overcoming the accuracy limitations of conventional markers.

LEAG provides rotation angle information around an axis based on the position of the black line. It comes in two types: O-LEAG (orthogonal LEAG) and P-LEAG (parallel LEAG), depending on the relationship between the axis of rotation and the direction of black line movement (Fig. 2). High-accuracy markers require attitude data around two orthogonal axes. Initially, with only O-LEAG available in the previous LentiMark, two LEAGs were arranged orthogonally. Subsequently, the development of P-LEAG enabled a parallel configuration of O-LEAG and P-LEAG, leading to the creation of the new high-accuracy marker, LentiMark-II [24](Fig. 3).

C. Feature dot

In LeagTag, we use the four feature dots as alternative feature points to the four corners, which are traditionally used in square-shaped markers, in order to enhance the accuracy of pose measurements. This is because the positions of the corners can vary due to lighting conditions or blurring, but the positions of the dot centers are less affected by these factors and can be extracted stably from the image. It has been reported that this approach improves the accuracy of pose measurements [25].

D. 2-D code

The role of the 2-D code is to enable initial detection of a marker and identification of the ID number. We use ArUco markers [5] as 2-D codes. In the case of elongated markers, we are compelled to make the size of the 2-D code relatively small. However, reducing the marker size adversely affects recognition accuracy and code identification accuracy. In the subsequent sections, we will discuss measures developed in LeagTag to mitigate this issue, as well as the placement of 2-D codes and the assignment of ID numbers.

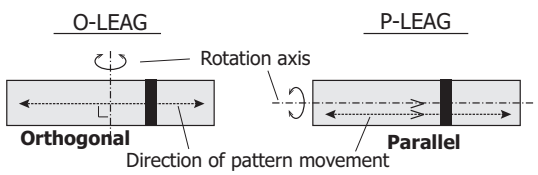

Fig. 2. Behaviour of O-LEAG and P-LEAG.

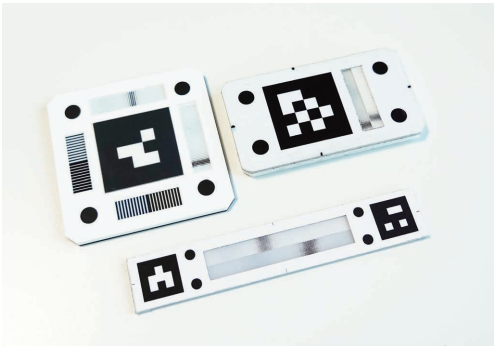

Fig. 3. High-accuracy fiducial markers. (top left) LentiMark, (top right) LentiMark-II, (bottom) LeagTag presented in this paper. The aspect ratios are 1.0, 1.8, and 5.6, respectively.

Up to this point, we have introduced the technology accumulated from our previous research. From here, we will discuss the development carried out in this study to achieve LeagTag, the world's first elongated high-accuracy marker.

E. Arrangement of Each Element in LeagTag

1) Relative size of LeagTag and LEAG: We will explain how we determined the relative sizes of LeagTag and LEAGs. We first considered the minimum size for LeagTag. Fig. 4 illustrates this concept. In the past, we developed a virtual stylus (digital pen) that tracked the pen tip using LentiMark-II (Fig. 4, left)[26]. However, due to its size and unwieldiness, as well as the fact that further downsizing of LentiMark-II is not feasible, we are considering replacing it with a smaller LeagTag in the future. The maximum marker size for the stylus is approximately 45x8mm. On the other hand, from the perspective of ensuring angular resolution and manufacturability, the current minimum length for LEAG is 20-22 mm, as previously used with LentiMark-II. Taking these constraints into account, the aspect ratio of the marker was set to approx. 5.6, and the length of the LEAG was approx. 0.5 times the length of the marker.

2) The arrangement and size of feature dots: The role of feature dots is to serve as feature points for calculating the marker's pose using the PnP solver, as well as reference points when reading the position of LEAG's black lines. Therefore, in one view, increasing the distance between feature dots improves pose estimation accuracy, while in the

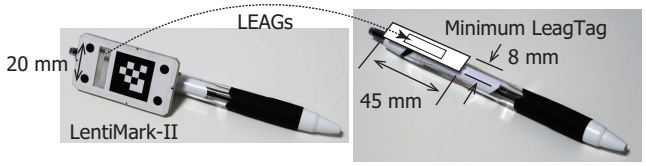

Fig. 4. The rationale behind determining the size of the smallest LeagTag and the proportion occupied by LEAG. We intend to apply LeagTag to a virtual stylus [26] in the future.

other view, it's preferred to have them closer to LEAG. To meet these requirements within a limited marker area, we positioned the feature dots as shown in Fig 1. The diameter of the dots is designed to be approximately the length of the diagonal of one cell of the 2-D code's matrix bit pattern. If they are smaller than that, it is possible that while the 2-D code is recognized on the image, the feature dots might not be recognized, and vice versa.

3) 2-D codes design and arrangement: As mentioned in II-D, the 2-D code for LeagTag tends to have a smaller size, which can result in a reduced recognizability distance. To extend the recognition distance even slightly for this issue, we made the matrix bit pattern inside the 2-D code coarser and increased the size of individual cells. Specifically, we changed the previously used 4x4 cell pattern to a 3x3 cell pattern. Since there is an additional black border of one cell around each matrix bit pattern, this change increases the length of one side of a cell from (1+4+1)/(1+3+1) = 1.2 times. Consequently, it is expected that the recognition distance will also increase by a factor of 1.2.

However, reducing matrix pattern resolution decreases available 2-D code ID numbers. To expand the pool of available ID numbers, we use two 2-D codes with ID assignment based on their combination. As depicted in Fig. 1, two 2-D codes are placed at each end of the marker. Separating the codes at marker ends, not adjacent, places feature dots and LEAGs between the two 2-D codes. This ensures full marker capture for pose measurement when the ID number is recognized at first. Also, placing codes close to feature dots enhances marker recognition accuracy as they are reference points for feature dot detection.

4) ID number assignment: Fig. 5 shows the definition of the coordinate system used in LeagTag and the rules for placing the 2-D code. ArUco markers have orientations and are positioned so that the upward direction is aligned with the Y+ direction of LeagTag. The main number code is placed on the X- side, while the sub-number code is placed on the X+ side. The ID numbers of LeagTag are assigned to pairs of two numbers (Main #, Sub-#). With each of them having 64 numbers assigned, a total of 64x64 = 4096 ID numbers can be used by combining them. When using one 4x4 code, the number of ID numbers was 1000. The greater the number of assignable ID numbers, the higher the versatility of the marker's applications.

III. Marker Measurement Algorithms

Just as with the design and development of physical markers, software development to maximize its performance is crucial. In this section, we will discuss the recognition and measurement algorithms for LeagTag, with a focus on the new developments conducted in this study.

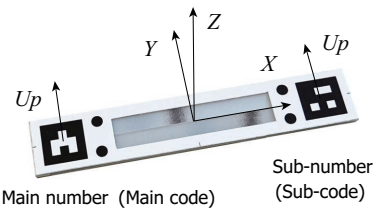

Fig. 5. LeagTag coordinate system and 2-D code placement.

A. Overview

The recognition and measurement algorithm of LeagTag is outlined as follows:

1) Detect all 2-D codes.
2) Search for pairs of 2-D codes, and detect LeagTag candidates.
3) Detect the feature dots, and calculate the initial pose (position and orientation).
4) Measure the LEAGs and correct the marker orientation.

The details for each item are described below.

B. Detect all 2-D Codes

Initially, all 2-D codes in the captured image are detected. Since the 2-D code used is ArUco marker [5], detection is performed using the ArUco software provided as part of the OpenCV library. In this study, two 3x3 codes are used instead of a 4x4 code high-accuracy marker used in previous studies. The "dictionary" for the 3x3 code is not provided by default, so it is necessary to create a dictionary file for the 3x3 code in advance and load it at program startup. Reference [27] can be helpful in this regard. In LeagTag, 3x3 codes that can assign 64 ID numbers are used.

C. Search for Pairs of 2-D Codes, and Detect LeagTag Candidates.

Identifying adjacent code pairs is relatively easy, but robustly identifying distant pairs posed a challenge. To achieve this, we first test all detected pairs of 2-D codes against multiple criteria and consider those that pass all of them as candidates for LeagTag. The criteria include size ratio, distance, orientation, and spatial positioning. If the pose estimation of individual 2-D codes were accurate, these tests could have been performed in 3-D space. However, due to limited accuracy in the pose estimation (cf. II-B), we conducted it in the 2-D space within the image. Fig. 6 illustrates a test result example for LeagTag candidate detection. The left figure shows a test pattern containing a potentially confusing sub-code. The correct code was successfully detected from multiple codes, resulting in the extraction of a LeagTag candidate (center figure). Feature dots were then detected (cf. III-D), validating the LeagTag's pose measurement (right figure).

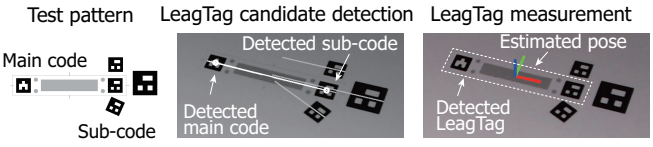

Fig. 6. An example of the results of "Search for pairs of 2-D codes and detect LeagTag candidates" test (center). The subsequent feature dots detection process and pose measurement process are also correctly carried out (right).

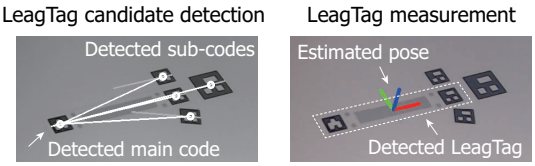

Fig. 7. An example of detection results when relaxing the detection criteria for LeagTag candidates (left). Subsequently, by using the feature dots detection process, one correct LeagTag can be recognized and measured from among multiple candidates (right).

For reference, Fig. 7 demonstrates the outcome when LeagTag candidate extraction conditions are relaxed. The left figure displays multiple incorrect candidates alongside the genuine LeagTag. However, only the correct candidate is verified as LeagTag and measured using the feature dots detection process (cf. III-D), as shown in the right figure.

D. Detect the Feature Dots, and Calculate the Initial Pose

Four feature dots are examined for their appropriate locations in the detected LeagTag candidates. Based on the 3-D pose of the main and sub-codes, regions are defined where two feature dots should exist on the right and left sides of each code (see Fig. 8). Due to the proximity between the 2-D code and feature dots (cf. II-E.3), the impact of 3-D pose estimation errors on calculating the search region is minimal.

Subsequently, blob detection is carried out within each binarized rectangular region, and specific criteria are applied to assess the presence of feature dots. This involves evaluating the area, circularity, and convexity of the extracted blobs near the region's center within certain predefined ranges. If all criteria are met, a feature dot is considered detected, and its centroid becomes the feature point's position. The presence of a LeagTag is confirmed when four feature dots are detected.

Now that we have the positions of the four feature points on the image, we can calculate the LeagTag's pose using the same PnP problem-solving method mentioned in II-B. This result serves as the initial pose, and if no further orientation correction using LEAG is conducted in the following steps, it will be the final measurement of the marker's pose.

E. Measure the LEAGs and Correct the Marker Orientation

The reading of LEAG value (position of the black line) is performed using the following steps (Fig. 9). First, a rectangular image of a certain size is created through perspective transformation using four feature dots to view LEAG from the front. Next, the brightness values of pixels are scanned along the long axis of LEAG, and pixels with brightness values in the top third of the ranking of darkness are extracted. Finally, the centroid of these pixels is calculated and taken as the LEAG value. With this algorithm, we can now obtain the position of black lines with sub-pixel accuracy. The angular resolution is approx. 0.2°. This process is performed similarly for both O-LEAG and P-LEAG. From two LEAG values, "visual-line angles [23]" around two axes can be obtained. These are used to correct the initial orientation and determine the final marker pose. The orientation correction method is the same as that described in [23] and [24].

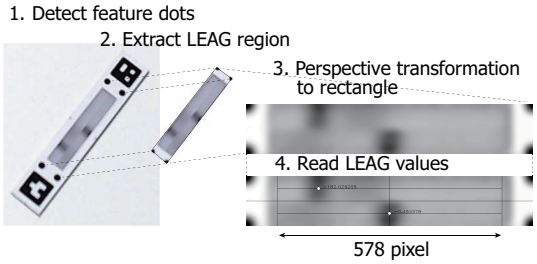

Fig. 9. Reading of LEAG values.

By the way, orientation correction is performed when the camera is within a cone with an approx. 50° vertex angle centered around the marker's perpendicular axis, in which the LEAG's black line is visible. Furthermore, no correction is applied to the marker's "position." The initial position, obtained using feature dots, is retained as the final position without any adjustments.

IV. Performance Evaluation of LeagTag

This section presents the results of evaluating the effectiveness and performance of LeagTag.

A. Measurement Environment

Fig. 10 depicts the measurement environment used in this study. The LeagTag test piece was affixed to a two-axis rotation stage, while the vision sensor utilized was the Grasshopper3 (GS3-U3-23S6M-C, FLIR Systems, Inc.) USB3.0 CMOS monochrome camera. The camera had an image resolution of 1280x720 pixels and an angle of view of 33.7°x19.3°. Mounted on a linear slider, the camera's distance from the marker could be continuously varied between 400 mm and 1500 mm. All processing was conducted on a laptop computer with the following specifications: a 64-bit CPU running at 2.11 GHz and 16 GB of RAM. The

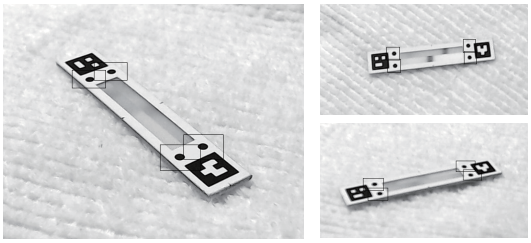

Fig. 8. Results of calculating the rectangular area with a feature dot based on the 3-D pose of the detected 2-D code.

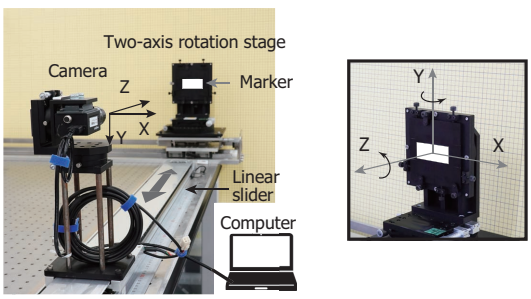

Fig. 10. Measurement environment.

code was written in the C/C++ programming language, and image processing was performed using the OpenCV 3.4 library. Under these specific environmental conditions, the measurement process could run at a speed of 25 FPS.

We defined the camera and marker coordinate system in accordance with Fig. 10. To alter the marker's orientation, we rotated a_Y [deg] around the Y axis and then a_Z [deg] around the Z axis. The marker's attitude after the change is represented as (a_Y, a_Z).

B. Ojective of Experiments

In the following experiments, we aim to demonstrate (1) LeagTag's efficient installation in tight spaces and its longer recognition distance compared to LentiMark (IV-C), (2) The potential for further extending this distance through 2-D code improvements (IV-D), and (3) LeagTag's pose estimation accuracy, which is equivalent to that of LentiMark (IV-E).

To clarify our experimental setup and position of our achevements, we would like to confirm the following points in advance: (i) In the conventional marker framework using the PnP method, pose estimation accuracy decreases as the marker size in the image decreases. (ii) Rectangular markers do not significantly improve orientation estimation accuracy, especially in the shorter dimension. (iii) The same applies when arranging square markers in a row to form a rectangular shape. (iv) Arranging multiple square markers does not affect the recognition rate of each individual marker.

C. Effect of Marker Shape

We investigated the effect of LeagTag's elongated shape, which can be installed in narrow spaces, on the marker recognition distance. In this experiment, we compared LeagTag with LentiMark because LentiMark is an active marker that falls under the same category of high-accuracy markers as LeagTag (LentiMark-II is no longer in use for various reasons). Fig. 11 shows LentiMark and LeagTag installed at their maximum size in a narrow space with a width of 10 mm and sufficient length. This assumes a flat space on the front of a convenience store shelf (Fig. 15). Note that the matrix bit pattern resolution of the 2-D codes for both markers was set to 4x4, for a fair comparison. We captured images of the two markers in Fig. 11 from the front and examined the maximum distance at which the markers could be recognized. The results, as shown in TABLE I, indicate that LeagTag can be recognized from a distance approximately 1.6 times greater than LentiMark. The main reason for this difference is the varying size of the 2-D codes for each marker. High-accuracy markers rely on successful 2-D code recognition as the starting point of their recognition process, and a failure at this stage leads to overall recognition failure. In this scenario, LeagTag's 2-D code had approximately 1.5 times the length of LentiMark's, enabling recognition from a greater distance.

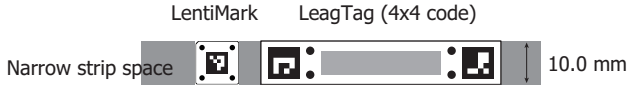

Fig. 11. Maximum sized LentiMark and LeagTag in a narrow space like a flat space in front of convenience store shelves.

TABLE I
MAXIMUM RECOGNITION DISTANCE OF MARKERS IN FIG. 11

LentiMark	LeagTag(4x4 code)
455 mm	735 mm

It has been confirmed that, when installed in a narrow space, a longer rectangular-shaped LeagTag has a longer recognition distance and is more practical than a square-shaped LentiMark.

D. Effect of Resolution of Matrix Bit Patten

Next, we investigated the effect of the resolution of the matrix bit pattern of a 2-D code on the marker recognition distance by measuring the maximum recognition distance for two types of LeagTag markers with different matrix pattern resolutions, as shown in Fig. 12. The result is shown in TABLE II. The LeagTag with a 3x3 code has a maximum recognition distance approximately 1.3 times longer than the 4x4 code LeagTag. While it differs slightly from the anticipated factor of 1.2 discussed in II-E.3, it can be assumed that recognition distance increases proportionally with cell size. Here, note that for the measurements of *B* and *C*, we used a lens with a wider angle of view than the one stated for *A* in order to fit the longest recognition distance within the movable range of the linear slider.

Combining the results of *B* and *C*, it can be concluded that when LentiMark and LeagTag are installed throughout a narrow space, LeagTag can be detected from more than twice the distance compared to LentiMark. Assuming the LeagTag from Fig. 12 (bottom) is installed on convenience store shelves, the recognition distance is sufficient given the typical aisle width of 900 mm.

E. Measurement Accuracy

We investigated the position and orientation measurement accuracy of LeagTag. The test piece is a LeagTag prototype shown in Fig. 1.

1) Orientation accuracy: We performed 3-DoF orientation measurement of a LeagTag, as illustrated in Fig. 10, while rotating it around the vertical axis of the rotation stage at an observation distance of 1008 mm. For each condition,

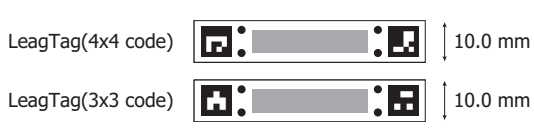

Fig. 12. Two types of LeagTag with different matrix pattern resolutions.

TABLE II
MAXIMUM RECOGNITION DISTANCE OF MARKERS IN FIG. 12

LeagTag(4x4 code)	LeagTag(3x3 code)
735 mm	955 mm

30 images were captured, and the mean and standard deviation of the mesured orientation were calculated. The results are presented in Fig. 13.

We compared the orientation error between the normal LeagTag (with LEAGs) and the case where LEAGs were not used (without LEAGs). The accuracy was evaluated by computing the absolute angle difference between the measured vector and the real vector of each coordinate axis (Fig. 13 left), and choosing the largest among the three. The standard deviations were also represented as error-bars.

Although it is known that pose measurement using feature dots (without LEAGs) has better accuracy than the conventional square AR marker [25], the orientation error is still significant in the frontal direction of the marker. On the other hand, using LEAGs was shown to reduce the error in the frontal direction. By switching to the measurement method that employs feature dots in the range of visual-line angles above 25°, it is possible to measure the orientation with uniformly high accuracy (error of about 0.5°) over a wide range of orientations. This is as accurate as previous high-accuracy markers [23][24] and significantly more precise than typical conventional markers (with an orientation error of up to 3 degrees or more) [22][28].

It should be noted that orientation error slightly increases as the rotation angle becomes larger. We believe that this is probably due to a slight tilt in the marker plane. When viewing the marker from an angle, the influence of the tilt is more likely to be apparent than when viewed from the front. By improving the manufacturing precision of the marker, it would be possible to improve pose measurement accuracy.

For reference, Fig. 14 (left) shows the relationship between distance and orientation errors. LEAGs provide stable orientation measurements even at extended observation distances.

2) Position accuracy: We examined the measurement error $(\Delta x, \Delta y, \Delta z)$ of the 3-DoF position while varying the distance from the marker. The result is shown in Fig. 14 (right). Due to the measurement principle, Δz is larger than Δx and Δy, which is a common characteristic of planar fiducial markers. At a distance of 1100mm, we observed a noticeable increase in the z-direction error, primarily due to image quantization error. This phenomenon is particularly evident in z-direction measurements, especially when the marker size on the image is small, during fiducial marker measurements. We can say from these results that the maximum position error is 0.25%, and the average position error is 0.09% (both including the error range). This is as accurate as previous high-accuracy markers [23][24]. Considering that the position error of conventional AR markers is over 1% [22], the position measurement of LeagTag is highly accurate. LEAGs are not involved in the position measurement, and this accuracy is attributed to the use of feature dots [25].

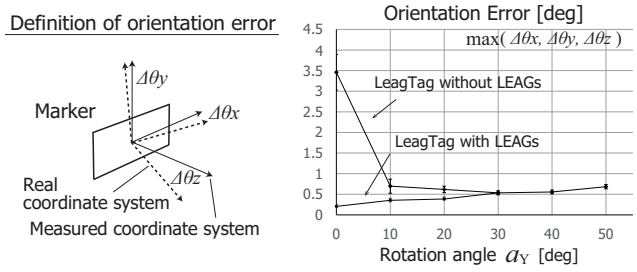

Fig. 13. Orientation measurement error. Distance: 1008 mm, Orientation: $(a_Y, 20.0)$. Pose measurement is possible even within the range of $a_Y > 50°$.

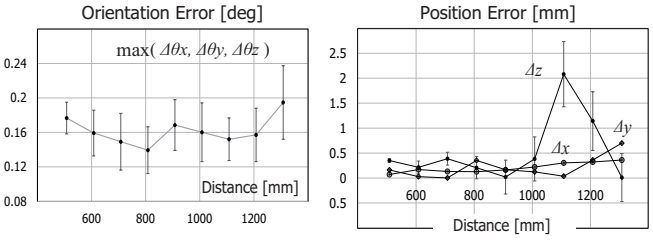

Fig. 14. (left) Relationship between distance and orientation error (Orientation: $(0.0, 0.0)$), (right) Position measurement error (Orientation: $(0.0, 0.0)$).

V. Possible Application Example

Fig. 15 shows the 2023 WRS Future Convenience Store Challenge. LentiMark was used to achieve precise alignment between the mobile manipulator and product shelves, replacing conventional markers with limited accuracy. However, the square-shaped LentiMark protrudes from the frame. LeagTag allows for installation in such tight spaces, as shown on the right side of the figure. This marker has the potential to support the autonomy of various robotic tasks in the future.

VI. Concluding Remarks

We have achieved a significant and world-first milestone by unveiling and successfully developing a method for creating high-accuracy, elongated fiducial markers. These markers were previously unattainable within the traditional framework of planar markers. While robots' ability to recognize and measure their environment through artificial intelligence has made remarkable progress, we believe that creating a robot-friendly environment using such fiducial markers is essential for robots to provide safer and more reliable services in human-robot coexistence spaces. Currently, we are working on developing technology to produce this marker at a lower cost and with higher quality.

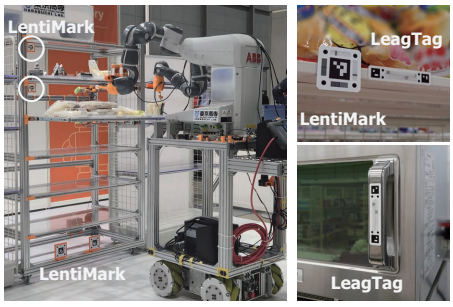

Fig. 15. (left) Example of utilizing LentiMark in WRS Future Convenience Store Challenge 2023. This image was provided by Haraguchi Lab., a participating team from the National Institute of Technology, Tokyo College. (right) Image of robot-friendly enhancement with LeagTag.

REFERENCES

[1] ARToolKit developer homepage, http://artoolkit.sourceforge.net/

[2] F. Bergamasco, A. Albarelli, E. Rodolà and A. Torsello, RUNE-Tag: A high accuracy fiducial marker with strong occlusion resilience, in Proc. IEEE Conf. Computer Vision and Pattern Recognition (CVPR), 2011, pp. 113–120.

[3] J. Wang and E. Olson, AprilTag 2: Efficient and robust fiducial detection, in Proc. 2016 IEEE/RSJ Int. Conf. Intelligent Robots and Systems (IROS), 2016, pp. 4193–4198.

[4] J. DeGol, T. Bretl, and D. Hoiem, ChromaTag: A Colored Marker and Fast Detection Algorithm,' In Proc. The IEEE Int. Conf. Computer Vision (ICCV), 2017, pp. 1472–1481.

[5] F. J. Romero-Ramirez, R. Muñoz-Salinas, R. Medina-Carnicer, Speeded up detection of squared fiducial markers, Image and Vision Computing, vol. 76, pp. 38–47, 2018.

[6] H. M. Balanji, A. E. Turgut, and L. T. Tunc, A novel vision-based calibration framework for industrial robotic manipulators, Robotics and Computer-Integrated Manufacturing, vol. 73, 102248, 2022.

[7] D. Hu, D. DeTone, and T. Malisiewicz, Deep ChArUco: Dark ChArUco Marker Pose Estimation. in Proc. 2019 IEEE/CVF Conf. Computer Vision and Pattern Recognition (CVPR), 2019, pp. 8428–8436.

[8] Y. Oba, K. Weaver, A. Parwal, H. Nagasue, and M. Fujishima, High-accuracy pose estimation method for workpiece exchange automation by a mobile manipulator, CIRP Annals, vol. 70, issue 1, pp. 357–360, 2021.

[9] Y. Zhang, G. Tian, and X. Shao, Safe and Efficient Robot Manipulation: Task-Oriented Environment Modeling and Object Pose Estimation, in IEEE Trans. Instrumentation and Measurement, vol. 70, pp. 1–12, 2021.

[10] A. de Oliveira Júnior, L. Piardi, E. G. Bertogna, and P. Leitão, Improving the Mobile Robots Indoor Localization System by Combining SLAM with Fiducial Markers, in Proc. 2021 Latin American Robotics Symposium (LARS), 2021, pp. 234–239.

[11] M. Kalaitzakis, B. Cain, S. Carroll, A. Ambrosi, C. Whitehead, and N. Vitzilaios, Fiducial markers for pose estimation. Journal of Intelligent & Robotic Systems, vol. 101, no. 4, 2021, pp. 1–26.

[12] J. Chen, C. Sun, and A. Zhang, Autonomous Navigation for Adaptive Unmanned Underwater Vehicles Using Fiducial Markers, in Proc. 2021 IEEE Int. Conf. Robotics and Automation (ICRA), 2021, pp. 9298–9304

[13] A. Khazetdinov, A. Zakiev, T. Tsoy, M. Svinin, and E. Magid, Embedded ArUco: a novel approach for high precision UAV landing, in Proc. 2021 Int. Siberian Conf. Control and Communications (SIBCON), 2021, pp. 1–6.

[14] D. Grewal, S. M. Noble, A. L. Roggeveen et al., The future of in-store technology, J. of the Academy of Marketing Science, vol. 48, pp. 96–113, 2020.

[15] Z. Tian et l., Polartag: Invisible data with light polarization, in Proc. the 21st Int. Workshop on Mobile Computing Systems and Applications, 020. pp. 74–79.

[16] M. D. Dogan et al., InfraredTags: Embedding Invisible AR Markers and Barcodes Using Low-Cost, Infrared-Based 3D Printing and Imaging Tools, in Proc. CHI Conf. Human Factors in Computing Systems, 2022, pp. 1–12.

[17] G. A. Garcia Ricardez et al.,Team NAIST-RITS-Panasonic at the Future Convenience Store Challenge, Keisoku to Seigyo, vol. 61(6), pp. 422–425, 2022.

[18] B. Mustafa et al.,DeepFormableTag: End-to-end Generation and Recognition of Deformable Fiducial Markers, ACM Transactions on Graphics, vol. 40(4), pp. 1–14, 2021.

[19] H. Uchiyama and H. Saito, Random dot markers, 2011 IEEE Virtual Reality Conference, 2011, pp. 35–38.

[20] V. Lepetit, F. Moreno-Noguer, and P. Fua, EPnP: An accurate O(n) solution to the PnP problem, Int. Journal of Computer Vision, vol. 81(2), pp. 155–166, 2009.

[21] G. Terzakis, and M. Lourakis, A consistently fast and globally optimal solution to the perspective-n-point problem, in Proc. European Conference on Computer Vision (ECCV), 2020, pp. 478–494.

[22] D. Abawi, J. Bienwald, and R. Dörner, Accuracy in Optical Tracking with Fiducial Markers:An Accuracy Function for ARToolKit, in Proc. the Third IEEE and ACM Int. Symp. Mixed and Augmented Reality (ISMAR), 2004, pp. 260–261.

[23] H. Tanaka, Y. Sumi, and Y. Matsumoto, A Visual Marker for Precise Pose Estimation based on Lenticular Lenses, in Proc. 2012 IEEE Int. Conf. Robotics and Automation (ICRA), 2012, pp. 5222–5227.

[24] H. Tanaka, and K. Ogata, A High-Accuracy Fiducial Marker with Parallel Lenticular Angle Gauges, in Proc. 2021 IEEE/RSJ Int. Conf. Intelligent Robots and Systems (IROS), 2021, pp. 8091–8096).

[25] H. Tanaka, K. Ogata, and Y. Matsumoto, Improving the Accuracy of Visual Markers by Four Dots and Image Interpolation, in Proc. 2016 IEEE Int. Symp. Robotics and Intelligent Sensors (IRIS), 2016.

[26] H. Tanaka, Turning Any Object into an Input Device with a High-Accuracy Fiducial Marker, 2022 IEEE/SICE Int.l Symp. System Integration (SII), 2022, pp. 975–976.

[27] Discussion in stackoverflow, OpenCV 3 and ArUco lib - Serialize Dictionary, https://stackoverflow.com/questions/35293750/opencv-3-and-aruco-lib-serialize-dictionary

[28] M. Kalaitzakis, S. Carroll, A. Ambrosi, C. Whitehead and N. Vitzilaios, Experimental Comparison of Fiducial Markers for Pose Estimation, 2020 Int. Conf. Unmanned Aircraft Systems (ICUAS), 2020, pp. 781–789.